All-normal-dispersion Yb-doped mode-locked fibre laser and its stability analysis

Kong Ling-Jie(孔令杰), Xiao Xiao-Sheng(肖晓晟), and Yang Chang-Xi(杨昌喜)†
State Key Laboratory of Precision Measurement Technology and Instruments, Department of Precision Instruments, Tsinghua University, Beijing 100084, *China*

(Received 5 December 2009; revised manuscript received 14 December 2009)

We experimentally demonstrate an all-normal-dispersion Yb-doped mode-locked fibre laser with no intentional spectral filter inserted. Pulses with 1.1 nJ pulse energy at a repetition rate of 20.4 MHz are achieved. A theoretical model of the fibre laser is derived, whose coefficients are explicitly dependent on the orientations of the wave plates and the polarizer. Based on the model, stability diagrams of both the mode-locking and the continuous wave regimes of the laser are presented. The influence of group-velocity dispersion (GVD) and cavity length on the stability of mode-locking is also discussed.

Keywords: fibre laser, mode-locking, ytterbium
PACC: 4255N, 4280W, 4280S

1. Introduction

Ultrashort optical pulses have great applications in fields such as ultrafast optics, optical fibre communication, optical measurement, micro-mechanism processing, and medical treatments.[1] Compared with mode-locked solid-state lasers, ultrashort pulse fibre lasers have advantages of compactness, greater stability and so on. So far, researchers have proposed soliton fibre lasers,[2] stretched pulse fibre lasers[3] and self-similar fibre lasers.[4,5] But the evolution mechanisms of these pulse fibre lasers fail in output pulse energy or complexness (as dispersion compensation components, such as prism pairs, grating pairs, chirp mirrors, and microconstruction fibres, are used). Recently, a novel all-normal-dispersion (ANDi) mode-locked fibre laser, in which all components are of normal dispersion, has been proposed.[6] In this diagram, the energy of output pulses can be much higher,[7−10] and designs can be greatly simplified especially for Yb-doped mode-locked fibre lasers whose operating wavelength is in the normal dispersion domain of common fibres.

Much work has been done on this novel ANDi fibre laser. Properties and mechanisms of ANDi fibre lasers have been studied extensively, and high pulse energy has been realized.[6−14] In most of the work a spectral filter is used to assist in stabilizing the mode-locking,[6−8] which also allows wavelength tuning. We have demonstrated an ANDi Yb-doped fibre laser with a birefringence filter, in which the central wavelength can be tuned across 46.3 nm, from 1024.5 to 1070.8 nm.[13,14] On the other hand, an ANDi pulse fibre laser with no filter inserted is demonstrated in Ref. [15], which is mode locked by a semiconductor saturable absorber mirror (SESAM). The SESAM may play the role of spectral filtering for chirped pulses. However, there are a number of drawbacks associated with employing SESAM, such as the slow recovery lifetime of SESAM being a barrier for achieving ultrashort pulses.

In this paper, we experimentally demonstrate an ANDi Yb-doped pulse fibre laser, mode-locked by nonlinear polarization rotation (NPR). It should be noted that there is no filter inserted in the cavity. It is the NPR that serves as a spectral filter and stablizes the mode-locking. Thus the laser cavity can be compacter. Pulses with 1.1 nJ pulse energy at a repetition rate of 20.4 MHz are achieved. Then a theoretical model of the fibre laser based on Ref. [16] is derived to analyse the stability of both the mode-locking and the continuous wave regimes of the laser under different orientations of the wave plates and the polarizer. We also discuss the influence of group-velocity-dispersion (GVD) and cavity length on the stability. The theoretical stability diagrams of the mode locking regime are presented.

2. Experiment setup and results

The experiment setup of the ANDi Yb-doped mode-locked fibre laser is shown in Fig. 1. The cavity length is about 9.78 m, and the average GVD is

†Corresponding author. E-mail: cxyang@tsinghua.edu.cn
© 2010 Chinese Physical Society and IOP Publishing Ltd

about 0.026 ps^2/m. The length of Yb-doped fibre, whose pump absorption is 250 dB/m at 975 nm, is 48 cm. The fibre isolator forces unidirectional ring operation. The pump is coupled into the cavity through a wavelength division multiplexer (WDM). Counter pumping is utilized to minimize residual pump, for the pump absorption is polarization-dependent in this schematic. With two quarter wave plates and one half wave plate, the polarization state could be adjusted for initializing and stabilizing mode-locking by NPR.[17] The polarization beam splitter (PBS) converts the nonlinear polarization rotation into amplitude modulation. The portion of the pulse diverted out of the the cavity by PBS serves as the output port.

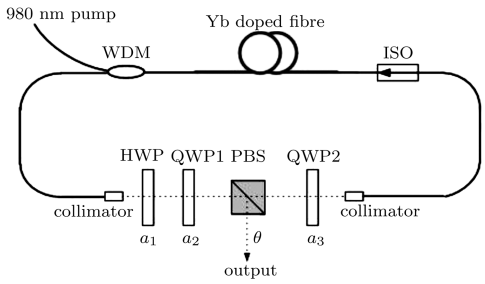


Fig. 1. Experimental setup. WDM: wavelength division multiplexer, ISO: isolator, HWP: half wave plate, QWP: quarter wave plate, PBS: polarization beam splitter.

It should be noted that no additional element for limiting the laser radiation spectrum is employed in this cavity, unlike Ref. [7]. In this case, the NPR serves as a saturable absorber, which has a slowly-decaying sinusoidal dependence of transmittance on intensity. The variation of the polarization state along the spectrum leads to a strong spectral filtering by the PBS.

With the pump power above the threshold (around 200 mW in our setup), the laser is self-starting after aligning the wave plates. Figure 2 shows the experimental results when the pump power is 425 mW. The output spectra in linear and logarithmic scales (the inset) are shown in Fig. 2(a). The central wavelength is 1033.8 nm, and the –20 dB bandwidth is 10.5 nm. The spectrum exhibits a characteristic shape with sharp peaks near its steep edges, which is induced by net normal dispersion of the cavity.[7,12] The asymmetric mode-locked spectra may be attributed to the third order dispersion of cavity.[18] The pulse train on digital sampling oscilloscope is shown in Fig. 2(b). It shows the repetition rate is 20.4 MHz, and the unequal intensity of the pulse train is due to digital sampling. The output power is 23 mW, thus the single pulse energy is about 1.1 nJ. Figure 2(c) shows the autocorrelation trace of the output pulses, which is measured with a long-range autocorrelator. It indicates that the full width at half maximum of the output pulse is about 15.6 ps under the assumption of a sech^2 temporal profile. These highly chirped pulses can be dechirped to near their transform-limited duration outside the cavity.[19]

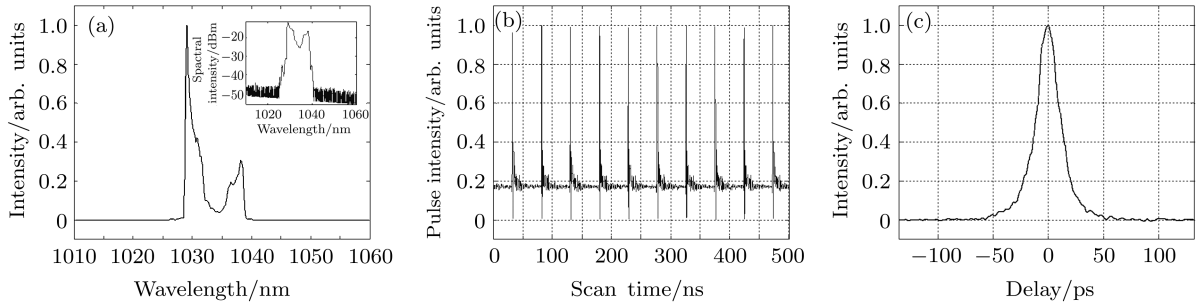


Fig. 2. Outputs of the laser. (a) spectra in linear and logarithmic scales (the inset), (b) pulse train, (c) autocorrelation trace.

3. Theoretical model

In experiments, the operating regimes and their stabilities depend greatly on the orientations of the wave plates. That is because adjusting the wave plates leads to a relative variation of the losses undergone by the wings and the centre of the pulse. So it is necessary to study the stability domains as a function of these angles.

Based on Leblond *et al*'s theory,[16] we derive a master equation to model the laser setup shown in Fig. 1. The resulting equation for electric field amplitude F, for a large number of round trips in the cavity,

is written as

$$\mathrm{i}\frac{\partial F}{\partial \varsigma} = \mathrm{i}g_1 F + \left(\frac{\beta_2}{2} + \mathrm{i}\rho\right)\frac{\partial^2 F}{\partial t^2} + (D_\mathrm{r} + \mathrm{i}D_\mathrm{i})F\,|F|^2\,, \quad (1)$$

where g_1 is referred to as the excess of linear gain, β_2 is the GVD coefficient, $\rho = g/w_\mathrm{g}$ is the gain filtering, $g = g_0 + \varepsilon g_1 + O(\varepsilon^2)$ is the gain efficient, and w_g is the spectral gain bandwidth. In order to compensate losses, g_0 must satisfy

$$g_0 = \frac{-1}{2L}\ln(\beta^2\,|Q|^2), \quad (2)$$

where β is the transmission coefficient of the polarizer. D_r and D_i are the real and the imaginary parts of $D = -P/(Q)$. The coefficients P and Q given in the appendix explicitly depend on the angles a_1, a_2, a_3, and θ. Here, we assume that the eigenaxes at both ends of the fibre are aligned and parallel to the x and the y-axes of the laboratory frame. As labeled in Fig. 1, a_1 (a_2, a_3) is the angle between the eigenaxis of the wave plate HWP (QWP1, QWP2) and the x-axis, and θ is the angle between the passing axis of the polarizer and the x-axis.

Apparently, Eq. (1) is of cubic complex Ginzburg–Landau (CGL) type. It admits stable analytical short pulses solution, and a criterion for mode-locking operation can also be given in the case of normal dispersion.[16,20] In the domain $D_\mathrm{i} < 0$, the modulation instability shows that the continuous wave (CW) operating regime is stable if the gain is sufficient. In the domain: $D_\mathrm{i} > 0$ and the excess of linear gain $g_1 < 0$, the localized solution may arise from noise spontaneously. This solution is not stable from the mathematical point of view, because the saturation of the gain, which limits the total energy in the cavity, will fix the number of pulses. While this number indefinitely increases in the frame of the cubic CGL equation, the saturation of gain is not taken into account by the model. In this case mode locking occurs. In the domain: $D_\mathrm{i} > 0$ and $g_1 > 0$, the modulation stability shows that the CW is not stable, and the localized solution broadens quickly.

4. Stability analysis

Based on the model above, the operating regimes of the laser as a function of the angles are presented below. As the number of degrees of freedom is large, it is difficult to carry out a systematic study of the stability of the solutions as a function of the angles. In the following, we generally fix some angles and vary the remaining ones. The stability diagrams show the regions of stability of both the CW and the mode-locked solutions. Similar discussions carried out in Refs. [16] and [20] show the advantages of the model in describing a real experiment. For the numerical computation, parameters are chosen as $w_g = 10^{13}$ s^{-1}, $A = 2/3$, $B = 1/3$, $K = 1.5$ m^{-1}, $\beta_2 = 0.026$ ps$^2 \cdot$m^{-1}, $L = 9.78$ m, and $\gamma = 3 \times 10^{-3}$ W$^{-1} \cdot$m^{-1}.

Figure 3 accords with Fig. 5 in Ref. [21], in which a unidirectional ring cavity containing a polarizer is placed between two sets of a half wave and a quarter wave plates. When ($a_2, a_3,\ \theta$) = (0°, 45°, 0°), the polarization that enters the fibre is circular as in our setup. As no NPR would occur in this case, there exists no mode-locking domain. In fact, the similar result can be obtained if $a_3 = \theta \pm 45°$.

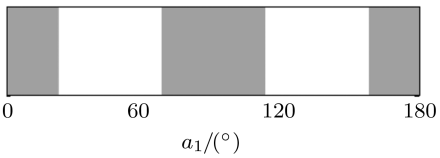


Fig. 3. Stability of the CW and the mode-locked solutions versus a_1 for ($a_2, a_3,\ \theta$) = (0°, 45°, 0°). White region: stable CW operation and unstable mode-locking, Light gray: unstable CW and unstable mode-locking.

The dependency of the operating regime of the laser on (a_1, a_3) is shown in Fig. 4. It is obtained for the orientations $(a_2, \theta) = (30°, 0°)$ of the quarter wave plate and the polarizer. As expected, the periodicity

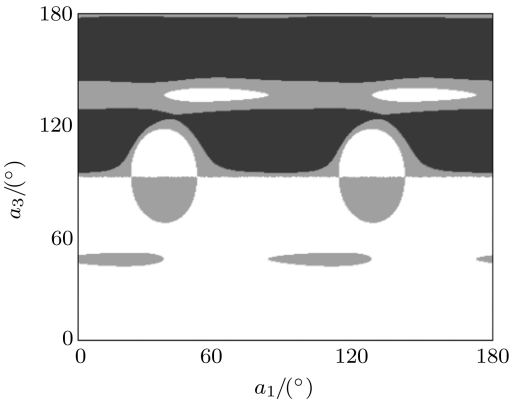


Fig. 4. Stability of the CW and the mode-locked solutions in the plane of (a_1, a_3) for (a_2, θ) = (30°, 0°). Dark gray: stable mode-locking operation and unstable CW. Other colours have the same meanings as those in Fig. 3.

versus a_1, the orientation of the half wave plate, is 90°. This can also be observed in Fig. 3. And the periodicity versus a_3, the orientation of the second quarter wave plate, is 180°. Note that when the orientations

of the second quarter wave plate are 45° and 135°, the conclusion in Fig. 3 still stands. It is shown that in this case, stable mode-locking operation depends more on a_3, the orientation of the quarter wave plate located before the fibre.

We explore the dependencies of the operating regimes of the laser on the orientations of the two quarter wave plates (a_2, a_3). Figure 5(a) is obtained for the orientations $(a_1,\ \theta) = (0°,\ 0°)$. And we find that the same diagram can be obtained as that for the orientations of $(a_1,\ \theta)$=(90°, 0°). But the contour plots of the effective nonlinear gain D_i as a function of the angles are different in these two cases. Thus they are not equivalent actually.

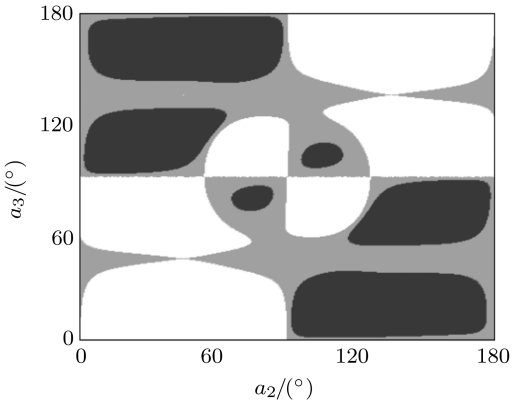


Fig. 5. Stability of the CW and mode-locked solutions in the plane of $(a_2,\ a_3\ )$ for $(a_1,\ \theta) = (0°,\ 0°)$ when GVD is 0.026 $\mathrm{ps}^2 \cdot \mathrm{m}^{-1}$. The colours have the same meanings as those in Fig. 4.

The influence of the orientation of polarizer θ on the operating regime of the laser for fixed orientations of the phase plates is shown in Fig. 6. Some representative results are presented here. The orientations of the wave plates (a_1, a_2, a_3) are (0°, 45°, 0°), (135°, 45°, 0°), and (30°, 0°, 30°) respectively in Figs. 6(a), 6(b), and 6(c). It can be obtained that the mode locking can be achieved by rotating the polarizer through any angle of the orientations of the phase plates as shown in Ref. [21].

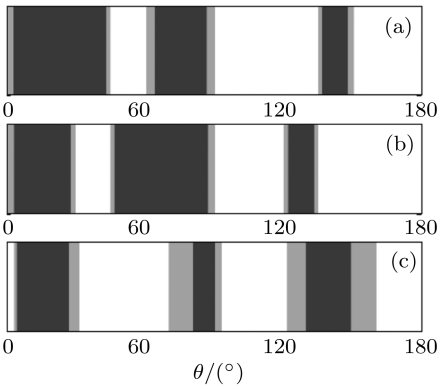


Fig. 6. Stability of the CW and the mode-locked solutions versus θ for (a_1, a_2, a_3) = (a) (0°, 45°, 0°), (b) (135°, 45°, 0°), and (c) (30°, 0°, 30°). The colours have the same meanings as those in Fig. 4.

Further, we study the influence of the GVD and the cavity length on the stability of the mode-locking solution. By increasing the GVD from 0.026 $\mathrm{ps}^2 \cdot \mathrm{m}^{-1}$ in Fig. 5 to 0.26 $\mathrm{ps}^2 \cdot \mathrm{m}^{-1}$ in Fig. 7(a), the stable mode locking regions enlarge, which accords with the predictions of the Haus's model.[20,22] As is well known, higher pulse energy can be achieved in a higher normal dispersion cavity.[12,18] Thus increasing the GVD not only benefits the stability but also enhances the pulse energy. Actually, the net cavity dispersion can also be increased by lengthening the fibre cavity. Comparing the stable mode locking regions in Fig. 7(b) with

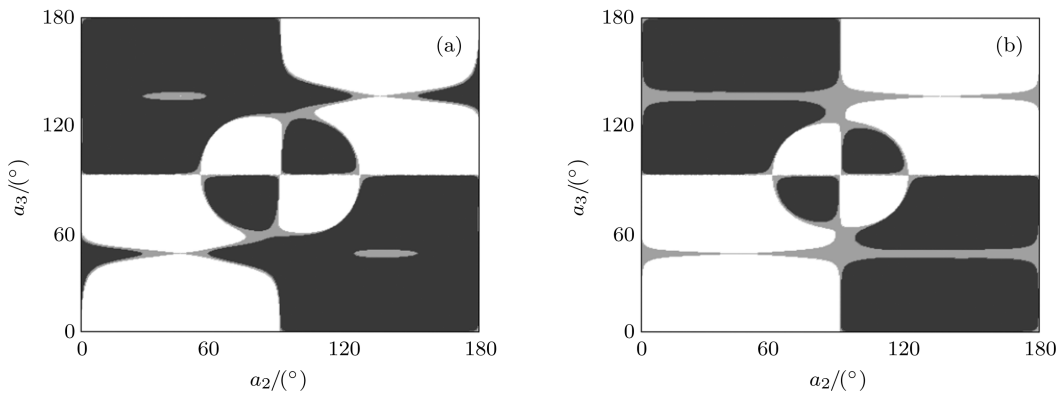


Fig. 7. Stability of the CW and mode-locked solutions in the plane of $(a_2,\ a_3\ )$ for $(a_1,\ \theta) = (0°,\ 0°)$ when (a) GVD is 0.26 $\mathrm{ps}^2 \cdot \mathrm{m}^{-1}$, $L = 9.78$ m; (b) GVD is 0.026 $\mathrm{ps}^2 \cdot \mathrm{m}^{-1}$, $L = 97.8$ m. The colours have the same meanings as those in Fig. 4.

those in Fig. 5, mode locking can be achieved more easily, which is also observed in our long cavity ANDi mode-locked fibre laser.[23]

5. Conclusion

We demonstrate an ANDi Yb-doped mode-locked fibre laser with no filter inserted. Pulses with 1.1 nJ pulse energy at a repetition rate of 20.4 MHz are achieved through NPR in a unidirectional ring cavity. The theoretical model based on our experiment setup is derived, and the stabilities of both the mode-locking and the continuous wave regimes of the laser under different orientations of the wave plates and the polarizer are analysed. The influence of GVD and cavity length on the stability is also discussed. Future work will be carried out to verify the theoretical model by experimental results further as done in Refs. [21] and [22].

Appendix

Coefficients in Eq. (1):

$$
\begin{aligned}
Q &= \mathrm{e}^{-\mathrm{i}KL}\frac{1}{2}\psi_1\chi_1 + \mathrm{e}^{\mathrm{i}KL}\frac{1}{2}\psi_2\chi_2,\\
P &= \mathrm{e}^{-\mathrm{i}KL}\frac{1}{4}\chi_1\Big\{\gamma[\psi_1|\psi_1|^2 + A\psi_1|\psi_2|^2]\frac{\mathrm{e}^{2gL}-1}{2g}\\
&\quad + B\gamma\psi_2^2\psi_1^*\,\mathrm{e}^{-3(g+\mathrm{i}K)L}\frac{\mathrm{e}^{(2g+4\mathrm{i}K)L}-1}{2g+4\mathrm{i}K}\Big\}\\
&\quad + \mathrm{e}^{\mathrm{i}KL}\frac{1}{4}\chi_2\Big\{\gamma[\psi_2|\psi_2|^2 + A\psi_2|\psi_1|^2]\frac{\mathrm{e}^{2gL}-1}{2g}\\
&\quad + B\gamma\psi_1^2\psi_2^*\,\mathrm{e}^{-3(g-\mathrm{i}K)L}\frac{\mathrm{e}^{(2g-4\mathrm{i}K)L}-1}{2g-4\mathrm{i}K}\Big\},\\
\chi_1 &= -\mathrm{i}\cos(\theta-2a_1) - \cos[\theta+2(a_1-a_2)],\\
\chi_2 &= \mathrm{i}\sin(\theta-2a_1) - \sin[\theta+2(a_1-a_2)],\\
\psi_1 &= \cos\theta - \mathrm{i}\cos(\theta-2a_3),\\
\psi_2 &= \sin\theta + \mathrm{i}\sin(\theta-2a_3).
\end{aligned}
$$

References

[1] Keller U 2003 *Nature* **424** 831
[2] Matsas V, Newson T, Richardson D and Payne D 1992 *Electron. Lett.* **28** 2226
[3] Haus H, Tamura K, Nelson L and Ippen E 1995 *IEEE J. Quantum Electron.* **31** 591
[4] Ilday F, Buckley J, Clark W and Wise F 2004 *Phys. Rev. Lett.* **92** 213902
[5] Deng Y, Tu C H and Lu F Y 2009 *Acta Phys. Sin.* **58** 3173 (in Chinese)
[6] Chong A, Buckley J, Renninger W and Wise F 2006 *Opt. Express* **14** 10095
[7] Chong A, Renninger W and Wise F 2007 *Opt. Lett.* **32** 2048
[8] Ruehl A, Kuhn V, Wandt D and Kracht D 2008 *Opt. Express* **16** 3130
[9] Liu B W, Hu M L, Song Y J, Chai L and Wang Q Y 2008 *Acta Phys. Sin.* **57** 6921 (in Chinese)
[10] Song Y J, Hu M L, Liu Q W, Li J Y, Chen W, Chai L and Wang Q Y 2008 *Acta Phys. Sin.* **57** 5045 (in Chinese)
[11] Chong A, Renninger W and Wise F 2008 *J. Opt. Soc. Am.* B **25** 140
[12] Wise F, Chong A and Renninger W 2008 *Laser & Photon. Rev.* **2** 58
[13] Kong L, Xiao X and Yang C 2009 *Conference on Lasers and Electro-Optics and the International Quantum Electronics Conference* Baltimore, Maryland, USA, May 31–June 5, 2009, paper JTuD70
[14] Kong L, Xiao X and Yang C 2010 *Laser Phys.* **20** 834
[15] Tian X, Tang M, Shum P, Gong Y, Lin C, Fu S and Zhang T 2009 *Opt. Lett.* **34** 1432
[16] Leblond H, Salhi M, Hideur A, Chartier T, Brunel M and Sanchez F 2002 *Phys. Rev.* A **65** 063811
[17] Luo Z C, Xu W C, Song C X, Luo A P and Chen W C 2009 *Chin. Phys.* B **18** 2328
[18] Chong A 2008 *Femtosecond Fiber Laser and Amplifiers Based on the Pulse Propagation at Normal dispersion* Ph. D Dissertation, Cornell University
[19] Kieu K, Renninger W H, Chong A and Wise F W 2009 *Opt. Lett.* **34** 593
[20] Haus H, Fujimoto J and Ippen E 1991 *J. Opt. Soc.* B **8** 2068
[21] Salhi M, Leblond H, Sanchez F, Brunel M and Hideur A 2004 *J. Opt.* A: *Pure Appl. Opt.* **6** 774
[22] Ortac B, Hideur A, Brunel M, Chartier T, Salhi M, Leblond H and Sanchez F 2003 *Appl. Phys.* B **77** 589
[23] Kong L, Xiao X and Yang C 2010 *Laser Phys. Lett.* **7** 359